Letters
IOP Publishing
Superconductor Science and Technology
Supercond. Sci. Technol. 31 (2018) 03LT02 (6pp)
https://doi.org/10.1088/1361-6668/aaa5de

Letter

Improvement of stability of Nb_3Sn superconductors by introducing high specific heat substances

X Xu[1], P Li[1], A V Zlobin[1] and X Peng[2]

[1] Fermi National Accelerator Laboratory, Batavia, IL 60510, United States of America
[2] Hyper Tech Research Incorporated, 539 Industrial Mile Road, Columbus, OH 43228, United States of America

E-mail: xxu@fnal.gov

Received 31 October 2017, revised 5 December 2017
Accepted for publication 8 January 2018
Published 24 January 2018

Abstract

High-J_c Nb_3Sn conductors have low stability against perturbations, which accounts for the slow training rates of high-field Nb_3Sn magnets. While it is known that adding substances with high specific heat (C) into Nb_3Sn wires can increase their overall specific heat and thus improve their stability, there has not been a practical method that is compatible with the fabrication of long-length conductors. In this work, we put forward a scheme to introduce such substances to distributed-barrier Nb_3Sn wires, which adds minimum difficulty to the wire manufacturing process. Multifilamentary wires using a mixture of Cu and high-C Gd_2O_3 powders have been successfully fabricated along this line. Measurements showed that addition of Gd_2O_3 had no negative effects on residual resitivity ratio or non-Cu J_c, and that flux jumps were remarkably reduced, and minimum quench energy values at 4.2 K, 14 T were increased by a factor of three, indicating that stability was significantly improved. We also discussed the influences of the positioning of high-C substances and their thermal diffusivity on their effectiveness in reducing the superconductor temperature rise against perturbations. Based on these results, we proposed an optimized conductor architecture to maximize the effectiveness of this approach.

Keywords: Nb_3Sn superconductor, stability, specific heat capacity

(Some figures may appear in colour only in the online journal)

1. Introduction

The instability of superconductors due to perturbations is a key issue for the design and operation of superconducting magnets. Efforts in developing Nb_3Sn dipole and quadrupole magnets in recent years show that Nb_3Sn magnets are less stable and have slower training rates than NbTi magnets: most Nb_3Sn dipole and quadrupole magnets require long trainings (e.g., tens of quenches) to reach 80%–90% of their short sample limits [1–3]. Magnet training is a very costly and time-consuming procedure; thus, it is very desirable to minimize it by improving the stability of superconducting magnets.

It is well established that for a superconductor with high critical current density J_c, improved intrinsic stability can be achieved by reducing filament size, increasing temperature margin, increasing specific heat, and dynamic cooling [4]. For modern high-J_c Nb_3Sn conductors used to generate high magnetic fields, there is limited room for further improvement of the first two factors. As to dynamic stabilization, Nb_3Sn coils are usually impregnated with epoxy, which has low thermal diffusivity, while common heat disturbances such as flux jumps and wire motions release substantial heat in short periods (0.01–1 ms), causing an adiabatic temperature rise before heat can be conducted away. On the other hand, increasing the specific heat of superconductors could not only

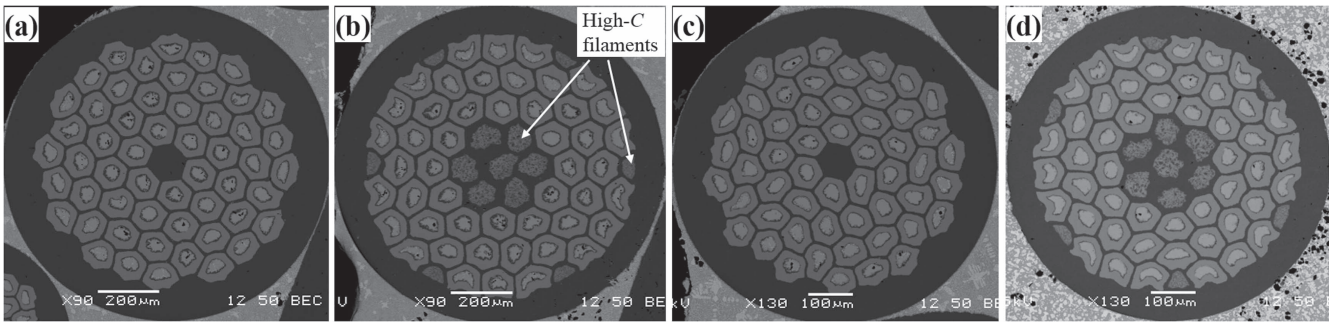

Figure 1. SEM images of (a) the control wire at 1.0 mm, (b) the high-*C* wire at 1.0 mm, (c) the control wire at 0.7 mm, and (d) the high-*C* wire at 0.7 mm.

lead to significant intrinsic stability gain, but also help to reduce sensitivity to external perturbations (i.e., improving energy margins against quenches). Due to the low specific heat C of Nb_3Sn conductors at their operational temperatures, even a tiny heat disturbance with energy of Q would cause a dramatic temperature rise ΔT, as $\Delta T = Q/C$. Therefore, improving conductor specific heat is one of the most promising approaches for improving magnet stability.

The specific heat of superconductors (such as NbTi and Nb_3Sn) and matrix (Cu) can hardly be significantly increased; however, there is a class of materials with high specific heat at low temperatures, and the addition of such substances to a superconducting wire in a proper architecture can improve its overall C [5–7]. Experiments have shown that the high specific heat of these substances was not fully utilized when they were added to epoxy, which has low thermal diffusivity [8]; however, when they were directly added into superconducting wires (e.g., being placed between the Ta barrier and the outside Cu sheath in bronze-process Nb_3Sn wires [9], or being filled into holes that were drilled in the Cu matrix in NbTi billets [10]), the minimum quench energies (MQE) of these conductors were significantly increased (e.g., by factors of five to seven as reported in [9]). Nevertheless, these schemes of adding high-*C* substances significantly increased billet fabrication difficulty and undermined wire drawability, making it difficult to obtain practical long-length wires. Furthermore, such schemes cannot be applied to distributed-barrier Nb_3Sn wires, which have high J_cs and are the conductors of choice for building high-field (10–16 T) accelerator magnets.

As discussed above, the key difficulty for practical use of this increasing-*C* technique lies in the proper modification of conductor design and fabrication to incorporate high-*C* substances without introducing much manufacturing difficulty. To solve this problem, we developed a technique to introduce high-*C* substances to distributed-barrier Nb_3Sn wires. To produce a present-day distributed-barrier Nb_3Sn wire, a number of hexagonal Nb_3Sn subelements (each with its own Cu sheath) and Cu rods are stacked into a Cu can to compose a billet, which is then drawn to wires at final sizes. Taking advantage of the stacking process, our scheme simply replaces some Cu rods and Nb_3Sn subelements with Cu tubes filled with high-*C* powders. This approach adds minimum difficulty to the wire manufacturing process.

Moreover, because high-*C* substances are typically ceramic compounds with very low thermal diffusivities, we also propose using a mixture of Cu and high-*C* powders instead of pure high-*C* powder. This brings two advantages: (1) Cu can enhance thermal conduction among the high-*C* particles, and (2) distributing ductile Cu in high-*C* particles (which are typically hard and non-deformable) benefits wire drawing and makes it easier to obtain small subelement size without filament breakage. The ideal structure for such a mixture is that Cu particles form a continuous network, which divides high-*C* powders into small islands (i.e., no larger than a few microns): in such a case, heat conduction distance in each high-*C* island is small, so it can absorb heat effectively in short periods.

2. Experimental

A 61-restack regular control wire and a high-*C* wire with filaments containing mixture of Cu and Gd_2O_3 powders (with the Cu:Gd_2O_3 weight ratio of 1:2) were fabricated. Their Nb_3Sn subelements were based on the 'tube type' technology: a Cu-encased Sn rod was inserted into a Nb-7.5 wt.%Ta tube to form a subelement—for such a subelement after heat treatment part of the Nb-7.5 wt.%Ta (~25%–30% of the whole subelement area [11]) would remain as a barrier against Sn leakage into the Cu matrix. Both wires were drawn to 1.0 mm and 0.7 mm diameters (with subelement sizes of ~100 μm and ~70 μm, respectively) with lengths over 100 m without any breakage, with SEM images shown in figure 1. The high-*C* filaments were placed both in the center and at the corners so that each Nb_3Sn subelement was not far from a high-*C* filament. The Cu/non-Cu ratios for the control wire and the high-*C* wire were ~1.0 and ~1.1, respectively (the high-*C* filaments were counted as 'Cu'). Gd_2O_3 was used for this work due to its commercial availability and high C at low temperatures. Cu powder of −325 mesh and nano Gd_2O_3 powder were used.

All wires (about 25 cm piece length) were heat treated at 625 °C for 250 h and at 640 °C for 200 h in an argon-flowing furnace. After heat treatment, the samples used for measurements and SEM studies were cut from the middle of the reacted wires.

For transport tests, each straight segment of ~5 cm was measured with field perpendicular to wire axis and voltage tap separation was 10 mm, with a criterion of 1 μV cm^{-1} used to determine its critical current (I_c). Residual resitivity ratio (RRR) measurements were done on ~6 cm long straight samples, and the RRR values were determined as the resistance at 300 K over that at 20 K. Magnetization versus magnetic field (*M-B*) loops were measured using the vibrating sample magnetometer option of a 9 T 'physical property measuring system' (PPMS). Each ~4 mm long wire sample was oriented with its axis perpendicular to the applied field. The heat capacities of the samples were measured in a PPMS from 2 K to 20 K at 0 T and 9 T. Minimum quench energies were measured on 1.0 mm wires. Strain gauges (WK-09-125BT-350 from micro-measurements) were glued to the samples using GE varnish, with the gauge patterns (~4 mm in length and ~1.5 mm in width) centered on the wires and their long sides parallel to the wire axes. After the complete curing of the GE varnish, the sample and the strain gauge were covered with a thick layer (~1 mm) of Stycast. A 400 W KEPCO power supply provided excitation voltage to the strain gauge. Using a LabView DAQ program, we can generate μs-wide pulse output from the power supply and measure the voltage across the strain gauge. With the I_c of the sample first measured, a constant bias current below I_c was applied to the sample and heat pulses were fired using the strain gauge. In this study, the duration of the heat pulses was fixed at 100 μs. A separate quench protection monitored the voltage across the sample and shut down the power supply if the quench threshold was reached. By gradually increasing the pulse power (in a step of 0.03 μJ when approaching the critical energy), the critical energy that induced a quench was defined as the MQE of the sample.

3. Results

The RRR values for the control wire and the high-*C* wire after reaction at 625 °C for 250 h were 107 and 271 for the 1.0 mm wires and 23 and 34 for the 0.7 mm wires, respectively, indicating that adding such high-*C* filaments did not undermine the RRR. The 4.2 K, 15 T J_cs normalized to the Nb_3Sn subelement areas of the control wire and the high-*C* wire after reaction at 625 °C for 250 h were 720 and 750 A mm^{-2}, respectively, which were similar. The heat capacity of a high-*C* filament after heat treatment at 625 °C for 250 h was measured in a PPMS and the calculated volumetric specific heat capacities of Gd_2O_3 at zero field and 9 T are shown in figure 2, along with the literature data for Cu and Nb_3Sn. It is seen that the addition of Gd_2O_3 is more efficient in increasing specific heat at 2 K than at 4.2 K. At 0 T, 2 K the ratio of the specific heat of Gd_2O_3 to that of Cu is nearly 1000, but it drops to only ~170 at 4.2 K. This is consistent with previous report that the specific heat of Gd_2O_3 with cubic crystal structure peaks at ~2 K [12].

The measured *M-B* loops at 4.2 K of 0.7 and 1.0 mm wires after reaction at 625 °C for 250 h are shown in figure 3. Compared with the control wires, the wires with high-*C* filaments had smaller flux jump amplitudes, indicating that the stability was improved. Larger flux jump amplitudes lead to higher energy release and temperature rise [13], and are very undesirable. It is also interesting to note that Gd_2O_3 has a large magnetic susceptibility at 4.2 K [14] and thus had non-negligible magnetization contributions to the *M-B* curves.

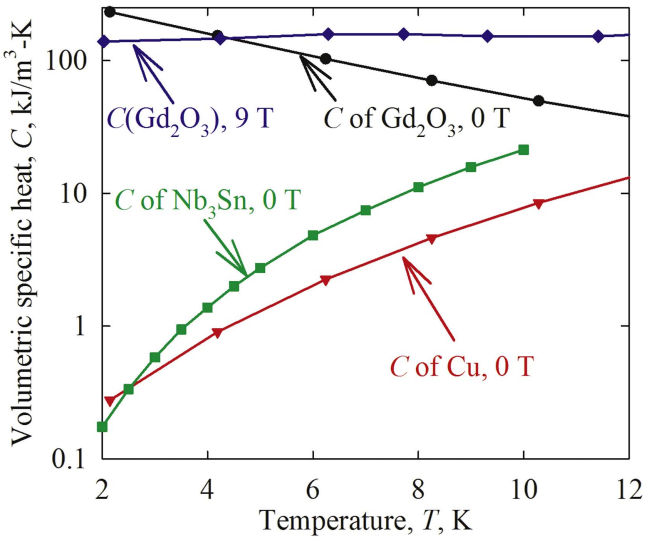

Figure 2. The volumetric specific heat of Gd_2O_3, Cu, and Nb_3Sn.

The MQE values of both 1.0 mm wires after reaction at 640 °C for 200 h were measured and the results are shown in figure 4. The I_cs at 4.2 K, 14 T of the control wire and the high-*C* wire were 444 and 426 A (with non-Cu J_cs of 1150 and 1180 A mm^{-2}), respectively. From figure 4 it can be seen that the MQE values of the high-*C* wire were over three times higher than those of the control wire.

4. Discussion

The reduced flux jumps in figure 3 reflect the improvement of stability in the low field range (<2 T), while the increased MQE values in figure 4 demonstrate the improvement of conductor stability at high fields against external perturbations while carrying high currents. These results show that the stability of Nb_3Sn conductors has been improved over a wide range of magnetic fields by introducing high-*C* filaments. It should be noted that an increase in *C* of Nb_3Sn conductors may lead to some change of normal zone propagation velocity, which needs further studies.

For the addition of high-*C* substances to improve the stability of superconductors, it is crucial to study their effectiveness in absorbing heat. We believe the effectiveness of high-*C* substances depends on two factors: their positions in a conductor, as well as their thermal diffusivities. In superconducting coils, heat is mostly generated by perturbations outside conductors (e.g., due to epoxy cracking) and transfer to the Cu matrix before diffusing into superconducting subelements. It is easy to understand that placing the high-*C* layer between the heat-exposed Cu matrix and the Nb_3Sn subelements is the most effective way to intercept the

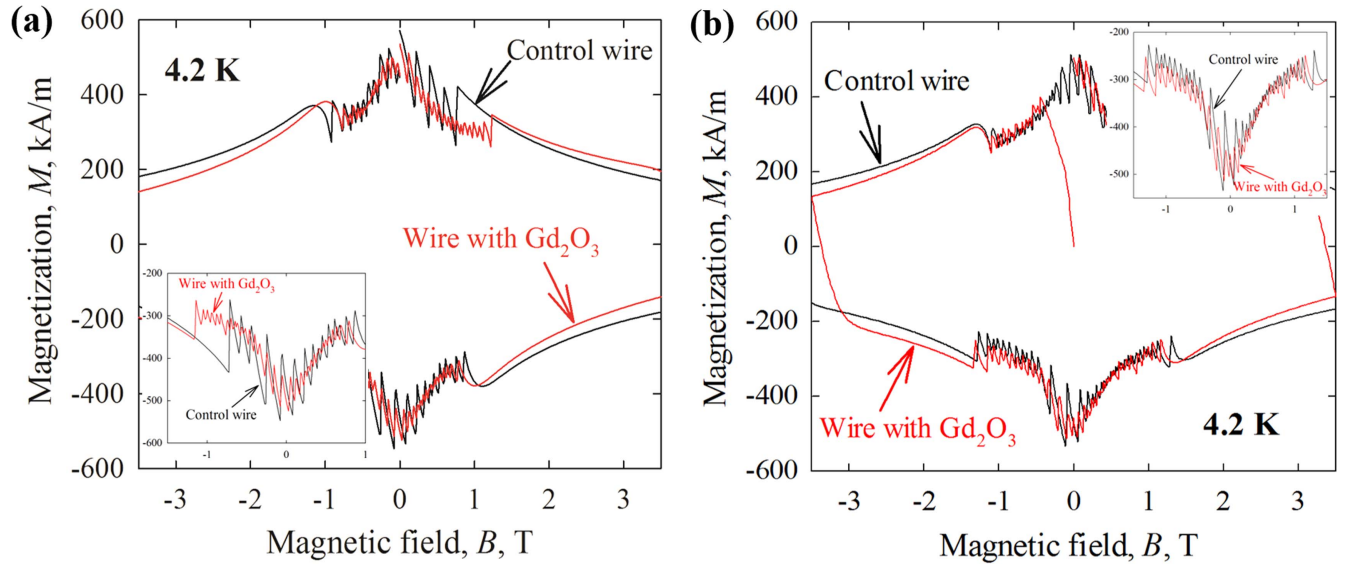

Figure 3. *M-B* loops of (a) 0.7 mm and (b) 1.0 mm wires (with magnetizations normalized to the non-Cu volumes). The inserts show blow-ups of the flux jump regions.

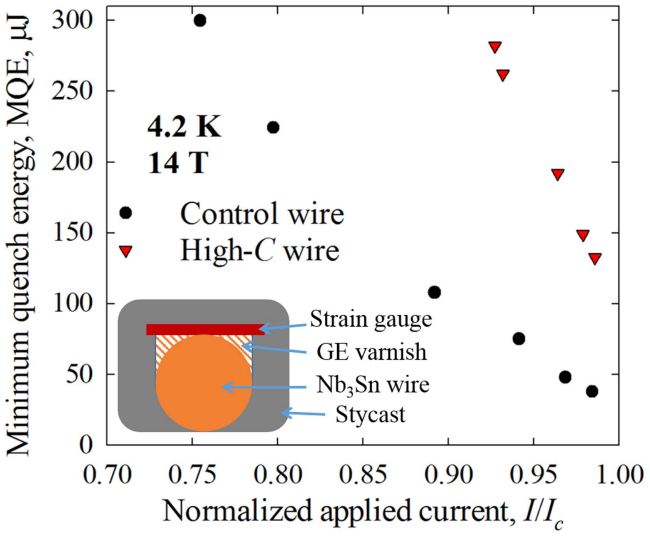

Figure 4. MQE values of the control wire and the high-*C* wire measured at 4.2 K, 14 T, with the insert showing a simple schematic diagram for measuring MQE.

heat before it diffuses into Nb_3Sn superconductors, while placing the high-*C* substances on the opposite side of the Nb_3Sn layer with respect to the heat source would have much less of an effect in preventing a temperature rise in Nb_3Sn.

Based on the above considerations, a feasible wire design to maximize the effectiveness of this technique is to place the high-*C* filaments in the outmost layer of the subelement array, a schematic shown in figure 5(b) (with a present-day Nb_3Sn wire in figure 5(a)). In this structure, the Cu sheath between the high-*C* filaments still allows for some heat diffusion from the outside Cu to inner-row subelements. In this case the effectiveness is sensitive to the thermal diffusivity of the high-*C* filaments: high thermal diffusivity is important to ensure quick heat absorption by the high-*C* substance. For example, if their thermal diffusivity is very low, a considerable portion of the heat can still diffuse into inner-row subelements because the time constant for heat absorption by the high-*C* filaments is too large.

Figure 6(a) shows an SEM image of a high-*C* filament used in the high-*C* wire in figure 1. We notice that Cu only formed isolated islands in Gd_2O_3 instead of forming the desired continuous thermal transport network. In such a case, the low thermal diffusivity of Gd_2O_3 does not allow heat to diffuse far into the high-*C* filaments over short periods; as a result, it is very likely that certain amount of Gd_2O_3 in the center of high-*C* filaments was not yet activated to absorb heat before flux jumps or quenches occurred. Figure 6(a) indicates that the Cu/Gd_2O_3 ratio (1:2) used in the high-*C* wire in this work might not be high enough. To determine the minimum amount of Cu powder to form a continuous heat transfer network, filaments with higher Cu/Gd_2O_3 ratios (2:1 and 4:1) were fabricated, with SEM images shown in figures 6(b) and (c), respectively. It can be seen that the Cu/Gd_2O_3 ratio of 2:1 still did not lead to a continuous Cu network, while the ratio of 4:1 was too high. Thus, we expect that the optimal Cu/Gd_2O_3 weight ratio may be around 3:1—this of course also depends on Cu and Gd_2O_3 particle sizes and mixing techniques. It is expected that new conductors with optimized Cu and Gd_2O_3 ratio and mixing and proper positioning of high-*C* filaments will have significantly superior stability compared with the high-*C* wire shown in this work.

With a Cu/Gd_2O_3 weight ratio of 3:1, it is estimated that for a Nb_3Sn conductor with 217 subelements and the outmost-layer subelements replaced by high-*C* filaments as shown in figure 5(b), the Gd_2O_3 takes ~2 vol.%, and the fraction of Nb_3Sn subelements depends on the Cu/non-Cu ratio design, while the rest is Cu (including the Cu matrix and the Cu powder in high-*C* filaments). With 2 vol.% of Gd_2O_3 added, the overall specific heat of a Nb_3Sn conductor can be improved by factors of ~20 and ~3.4 at 2 K and 4.2 K, respectively. It is worth pointing out that the addition of high-*C* filaments does not necessarily lead to a decrease in the Nb3Sn fraction thus

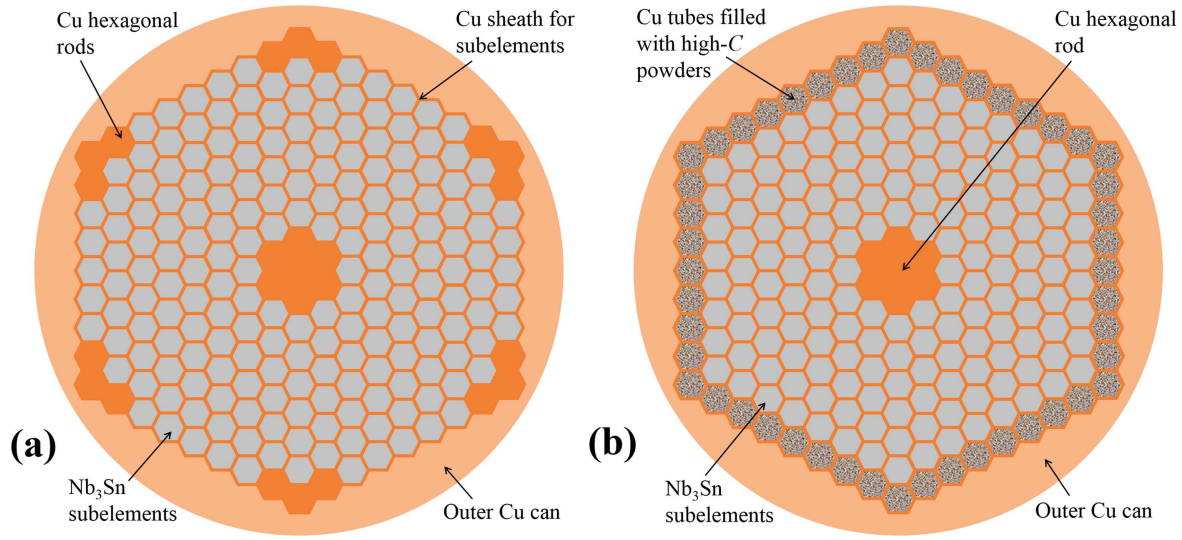

Figure 5. Schematics of cross sections of (a) a regular Nb_3Sn wire and (b) a wire with high-*C* filaments in the outermost layer.

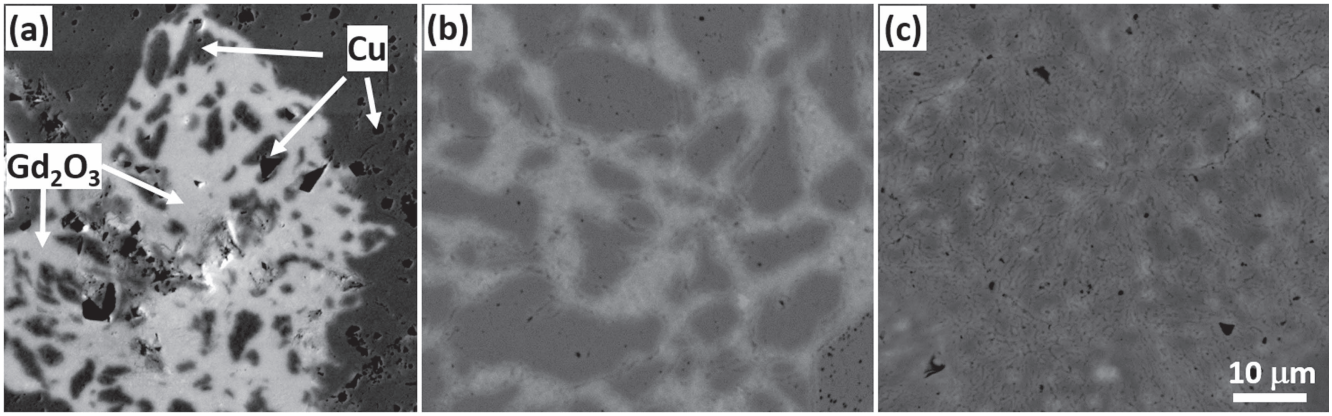

Figure 6. SEM images of Cu and Gd_2O_3 mixtures with Cu/Gd_2O_3 weight ratios of (a) 1:2, (b) 2:1, and (c) 4:1. In these images Cu appears as the dark phase and Gd_2O_3 appears bright.

engineering J_c, because we can reduce the Cu matrix volume to compensate for the addition of high-*C* filaments. For addition of 2 vol.% of Gd_2O_3, 1 kg of Nb_3Sn wire needs 17 grams of Gd_2O_3. Based on our investigations on the market, the price of Gd_2O_3 is significantly lower than the current price of Nb_3Sn conductors. In addition, the fabrication of such high-*C* filaments is based on the common powder-in-tube technique. Thus, it is expected that the prices of such new high-*C* conductors should not be noticeably higher than those of present-day Nb_3Sn conductors. Apart from Gd_2O_3, it is also useful to explore other high-*C* substances that have not only high *C*, but also high thermal diffusivity, such as PrB_6, which may work more effectively than Gd_2O_3.

5. Conclusions

An innovative technique was developed to introduce high-*C* substances to distributed-barrier Nb_3Sn superconductors without negative impacts on wire manufacturing. Conductors have been successfully fabricated with the addition of Gd_2O_3 without any issues. It was found that the RRR or non-Cu J_c were not negatively affected by the addition of Gd_2O_3. Measurements at 4.2 K showed that flux jumps at low fields were remarkably suppressed and MQE values at high fields were increased by a factor of three, indicating that the wire stability was significantly improved due to the addition of such high-*C* substances. The conductors in this work still have a lot of room for improvement. With further optimization of wire design, this new type of Nb_3Sn conductor can be industrially produced and used for large-scale applications to reduce or eliminate the training of Nb_3Sn magnets.

Acknowledgments

This work was supported by Fermi Research Alliance, LLC, under contract No. DE-AC02-07CH11359 with the US Department of Energy. The heat capacity measurements were conducted in the Center for Nanoscale Materials, Argonne National Laboratory, which was supported by the US Department of Energy, Office of Science, Office of Basic Energy Sciences, under Contract No. DE-AC02-06CH11357.

ORCID iDs

X Xu https://orcid.org/0000-0003-2728-5854

References

[1] Feher S *et al* 2007 Development and test of LARP technological quadrupole (TQC) magnet *IEEE Trans. Appl. Supercond.* **17** 1126–9

[2] Chlachidze G *et al* 2013 Test of optimized 120 mm LARP Nb_3Sn quadrupole coil using magnetic mirror structure *IEEE Trans. Appl. Supercond.* **23** 4001605

[3] Zlobin A V *et al* 2015 11-T Twin-aperture Nb_3Sn dipole development for LHC upgrades *IEEE Trans. Appl. Supercond.* **25** 4002209

[4] Wilson M N 1983 *Superconducting Magnets* (Oxford: Oxford University Press) pp 139–41

[5] Hancox R 1968 Enthalpy stabilized superconducting magnets *IEEE Trans. Magn.* **4** 486–8

[6] Russenblum S, Sheinberg H and Steyert W A 1977 High specific heat metals for use in superconducting magnets *IEEE Trans. Magn.* **MAG-13** 834–5

[7] Kwasnitza K, Barbisch B and Hulliger F 1983 Metallic materials for superconductor stabilization with very high specific heat and good thermal conductivity *Cryogenics* **23** 649–52

[8] Alekseev P A *et al* 2006 Influence of high heat capacity substances doping on quench currents of fast ramped superconducting oval windings *Cryogenics* **46** 252–5

[9] Keilin V E *et al* 2009 Considerable stability increase of Nb_3Sn multifilamentary wire internally doped with a large heat capacity substance (PrB_6) *Supercond. Sci. Technol.* **22** 085007

[10] Keilin V E *et al* 2012 Stability of superconducting coils made of NbTi wires internally doped with large heat capacity Gd_2O_3 powder *Supercond. Sci. Technol.* **25** 115017

[11] Xu X, Sumption M D, Bhartiya S, Peng X and Collings E W 2013 Critical current densities and microstructures in rod-in-tube and Tube Type Nb_3Sn strands—present status and prospects for improvement *Supercond. Sci. Technol.* **26** 075015

[12] Stewart G R, Barclay J A and Steyert W A 1979 The specific heat of C-phase Gd_2O_3 *Solid State Commun.* **29** 17–9

[13] Xu X, Sumption M D and Collings E W 2014 Influence of heat treatment temperature and Ti doping on low-field flux jumping and stability in $(Nb\text{-}Ta)_3Sn$ strands *Supercond. Sci. Technol.* **27** 095009

[14] Miller A E, Jelinek F J, Gschneidner K A and Gerstein B C 1971 Low-temperature magnetic behavior of several oxides of gadolinium *J. Chem. Phys.* **55** 2647–8